# Personalized Wearable Ankle Robot Using Modular Additive Manufacturing Design

Inigo Sanz-Pena , Hyeongkeun Jeong , and Myunghee Kim

Abstract—Wearable assistive robots can potentially improve the gait of individuals with reduced mobility. To address each individual's unique needs, personalized robots are necessary. In addition, robots equipped with portable systems are required to ensure their practical use in clinical and outdoor settings. We developed and evaluated a modular robotic ankle-foot orthosis (AFO) with two degrees of freedom and a portable actuation system, providing ankle plantarflexion and in/eversion assistance. The performance was evaluated via benchtop testing and human subject experiments. The benchtop testing demonstrated that the device could deliver 40 Nm of plantarflexion torque and 16 Nm of in/eversion torque, with rise times of 70 ms during plantarflexion, 84 ms during inversion, and 77 ms during eversion. The torque control bandwidth was greater than 13 Hz in plantarflexion and in/eversion. When a human subject used the device for squat assistance, the device presented its ability to track the desired torque trajectory with a maximum mean RMS error of 2.9  $\pm$  1.2 Nm for plantarflexion assistance and 0.7  $\pm$  0.5 Nm for in/eversion assistance. This study shows the potential of the proposed modular AFO, fabricated solely via additive manufacturing and utilizing an off-board portable actuation system. The proposed device can personalize ankle exoskeletons and examine in/eversion assistance effects for individuals with reduced mobility.

Index Terms—Additive manufacturing, ankle foot orthosis, exoskeleton, personalized design, wearable robot.

# I. INTRODUCTION

VER the last 30 years, diseases affecting the mobility of adult groups above 50 years old were among the ten with the most increases in disability-adjusted life years (DALYs) [1]. Motor disabilities can result in walking alterations and motor impairments [2]. Musculoskeletal disorders, stroke, and diabetes are the most common cause of limited mobility in

Manuscript received 25 February 2023; accepted 13 June 2023. Date of publication 28 June 2023; date of current version 7 July 2023. This letter was recommended for publication by Associate Editor A. L. Trejos and Editor J.-H. Ryu upon evaluation of the reviewers' comments. This work was supported in part by the National Institute for Occupational Safety & Health and National Science Foundation under Grant SES-2024863, and part by U.S. Army Research Lab under Grant W911NF-21-2-0230. (Inigo Sanz-Pena and Hyeongkeun Jeong contributed equally to this work.) (Corresponding author: Myunghee Kim.)

This work involved human subjects or animals in its research. Approval of all ethical and experimental procedures and protocols was granted by the Institutional Review Board from The University of Illinois at Chicago under Application No. 2020-0563, and performed in line with the principles of the Declaration of Helsinki.

The authors are with the Department of Mechanical and Industrial Engineering, University of Illinois, Chicago, IL 60607 USA (e-mail: isanzpen@uic.edu; hjeong29@uic.edu; myheekim@uic.edu).

This letter has supplementary downloadable material available at https://doi.org/10.1109/LRA.2023.3290529, provided by the authors.

Digital Object Identifier 10.1109/LRA.2023.3290529

people living alone [3]. Gait rehabilitation aims to improve function and regain mobility through physical therapy, including over-ground assisted walking, body-weight-supported training [4], and gait treadmill training, which can improve walking speed and endurance in chronic stroke survivors with the ability to walk independently [5]. However, physical therapy resources are often limited and sometimes unsuitable to the patient's walking dependency, rehabilitation intensity, and frequency requirements [6]. Wearable assistive robots are a technology to aid physical therapy methods for gait training that can reduce the effort of therapists and improve personalizing the rehabilitation [7]. Robot-assisted Gait Training can improve balance and independence in daily activities [8], lower limb function, and increase walking speed [9].

# A. Personalization of Wearable Ankle Robots

Wearable robots, in particular, robotic ankle-foot orthoses (AFO), have been used in gait assistance and rehabilitation in adults with disabilities affecting mobility [10], [11], [12]. The use of assistive technologies provides personalization of the rehabilitation based on the patient's characteristics and conditions. Personalization of wearable robots has been mainly centered around investigating subject-specific assistance control strategies using biofeedback to adapt to the high inter-subject variability and balance-related effort [9], [13], resulting in improved energy efficiency [14], [15]. Personalizing the mechanical design in wearable robots is also essential to accommodate anthropometry and gait biomechanics, considering the device functionality based on the user's condition and gait training aims [16]. Besides the current approaches to personalize the assistance control, there is a need to define a practical design to prescribe personalized exoskeletons for each user, considering inter-subject variability of anthropometry measures, ankle joint biomechanics and stiffness [17], and condition-related gait characteristics [16]. Modular wearable designs can be easily adapted to match the wearer's anthropometry [18] and could be a versatile approach to increase personalization capabilities.

## B. Ankle In/Eversion Torque Assistance

Aging affects ankle strength and range of motion, resulting in loss of stability, reduced ankle plantarflexion strength, and decreased eversion range of motion [19]. Several risk factors, including muscular weakness, loss of balance control, gait abnormality, and dementia, are linked to falls in the elderly [20]. The ankle torque strength and range of motion can affect balance

U.S. Government work not protected by U.S. copyright.

[19]. Ankle eversion taping can improve static and dynamic balance [21], and in/eversion assistance has reduced effort associated with balance in individuals with below-knee amputation [13]. The in/eversion assistance in a robotic AFO has been recently emphasized to improve muscle strength, promote a more comprehensive gait rehabilitation, including balance [9], and mitigate injury risk [22]. Implementing ankle in/eversion assistance in AFO could increase the capabilities of wearable robots during gait rehabilitation and training of elderly populations.

# C. Portable Emulator and Actuation Systems

Clinical rehabilitation sometimes requires equipment easily adapted to the rehabilitation setting and the patient's condition environment. Furthermore, space limitations have led wearable robots to create portable, independent control and feedback units. Portable off-board emulator systems have been developed to control soft exosuits [23], [24] and ankle foot prostheses [25]. However, these systems operate as stationary systems, which constraints the wearable robots' use in the laboratory. Portable onboard systems remove the stationary limitations and can expand their use in outdoor environments [26], [27], which could be beneficial in reducing patients' travel time to the clinic lab and increasing the accessibility to wearable assistive robots. A portable system with onboard and off-board capabilities can help improve the accessibility of AFO. Besides assisting in different indoor and outdoor environments, the off-board emulator setting allows the removal of the payload effects of the portable system, which could be required in the clinical setting.

# D. Aim of the Study and Proposed Device

The personalization of robotic AFO's mechanical design can further enhance the assistance benefits. Wearable ankle robots have been predominantly focused on plantar/ dorsiflexion assistance, limiting the potential outcomes and translational research. This study focused on developing a portable and modular robotic AFO using additive manufacturing and evaluating its performance as an emulator off-board system during human subject experiments. The AFO allows design personalization based on the subject's anthropometrics and ankle biomechanics with two active degrees of freedom (DOF), providing plantarflexion and in/eversion assistance.

## II. MODULAR ANKLE FOOT ORTHOSIS

## A. Mechanical Design

We developed a modular robotic AFO with active plantarflexion and in/eversion fabricated using additive manufacturing. The maximum plantarflexion and dorsiflexion ranges are 25° and 40°, respectively. A dual cable-transmission portable system was developed to provide plantarflexion and in/eversion assistance. Passive dorsiflexion is provided using two elastic rubber bands. The actuation was done using two independent cable-pulling transmissions driven by electric motors attached to the AFO's foot component (Exo-Talus) on the medial and lateral sides.

The modular AFO comprises four sub-assemblies (Fig. 1). The subassembly corresponding to the AFO's foot (Exo-Foot)

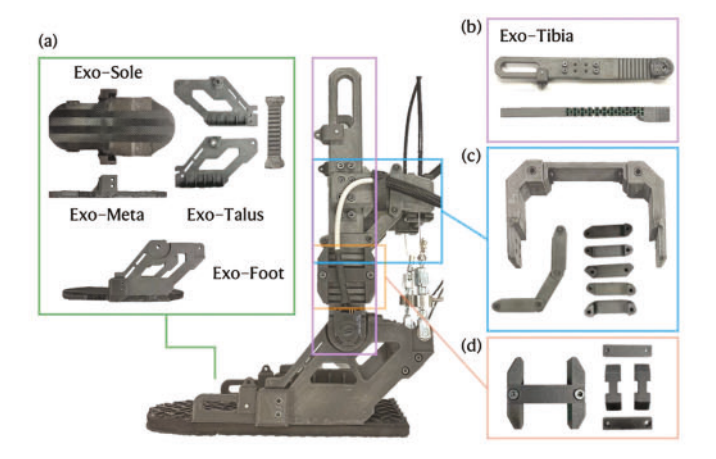


Fig. 1. AFO's modular components. (a) The exo-foot can be personalized for different shoe sizes, varying the length (exo-meta and exo-sole) and width (exo-sole), maintaining the exo-talus across sizes. (b) The exo-tibia is divided into three components. The most distal component holds the strap attaching the AFO to the subject's leg. The exo-tibia compliance in the frontal plane allows inversion and eversion thanks to its most proximal component. Both components are connected by a bolted part in between. (c) The connectors between the left and right exo-tibia and support components. (d) The component increases stiffness in the sagittal plane while allowing a range of motion in the frontal plane.

is composed of two main components, the Exo-Talus, and the Exo-Meta, connected using bolted joints (Fig. 1(a)). The medial and lateral components are joined through a rubber sole of medium stiffness that can be easily replaced to fit different shoe sizes. On the posterior side, a transversal component is used to connect both sides (Fig. 1(a)), providing high compression stiffness in the medial-lateral direction while allowing the in/eversion compliance of the device. At the AFO ankle joint, the Exo-Tibia assembly is coupled using a hinge joint.

The Exo-Tibia is divided into three components (Fig. 1(b)). One proximal to the ankle joint, which is a parametric lattice structure to personalize the in/eversion compliance in the frontal plane, one distal component that is used to connect the AFO to the wearer's shank, and a bolted connecting part in the middle that is used to hold and route the cable transmission. This part transmits the assistive torque during squatting activities. Implementing a compliant structure at the ankle joint reduces the kinematic constraints in the frontal plane presented by the AFO-human interface characteristics at the foot. The Exo-Tibia of the left and right sides are connected on the posterior side using a bridge component. The components connected to the Exo-Tibia hold and route the cable transmission (Fig. 1(c)). This is the main component that transmits the assistive torque to the subject's tibia during sit-to-stand.

To reduce the torque dissipation, support components are used to strengthen the Exo-Tibia in the sagittal plane while allowing the ankle's frontal plane range of motion (Fig. 1(c) and (d)). The attachment of the AFO to the subject's leg is performed using a strap located at the anterior tibialis. To maximize the assistive torque transmitted to the subject while maximizing comfort, the AFO is attached to the subject's leg at 1/3 of the tibia distance from the anterior origin, coincident with the most anterior part of the tibialis anterior and avoiding the interface of the Exo-Tibia

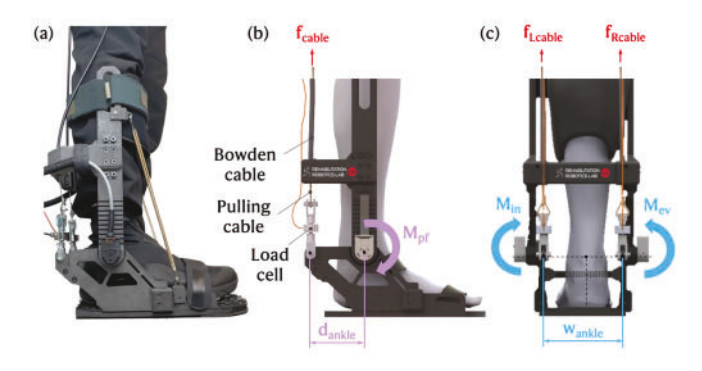


Fig. 2. (a) Subject wearing the AFO on the right leg; (b) and (c) represent the moment arms, and force control components for plantarflexion and in/eversion assistance, respectively.

with the knee. We used cushioned protection on the anterior, posterior, medial, and lateral sides of the tibia, maintaining the Exo-Tibia straight when attached to the subject.

The AFO can be easily personalized for different subjects by changing the Exo-Meta and Exo-Sole depending on the foot size (length and width). To fit the subject's leg length, the AFO only requires changing the most distal component of the Exo-Tibia (Fig. 1(b)), allowing the personalization based on shoe size and height of subjects by just printing two components and the rubber of the Exo-Sole (Fig. 1(a)). We used additive manufacturing to implement lightweight components that can be personalized and allow leg anthropometric and ankle biomimetic configurations using parametric designs. The components were manufactured in nylon-carbon fiber N12 Carbon Fiber using a Method-X fused filament printer (*Ultimaker*, *Netherlands*) (Fig. 1(c)). The weight of the AFO is approximately 0.9 kg.

The main components located at the AFO for the assistance control and transmission of the forces as well as the torques notation, are represented in Fig. 2. The plantarflexion torque  $M_{pf}$ , is defined as the sum of the left and right toe torques. Similarly, the in/eversion torque  $M_{in-ev}$ , was defined as the difference between the left and right toe torque multiplied by a constant defined by the geometry [28].

$$M_{pf} = M_L + M_R$$
 
$$M_{\text{in-ev}} = (M_L - M_R) \cdot \frac{w_{ankle}}{2d_{\text{ankle}}} \tag{1}$$

## B. Portable Actuator System

The AFO has two incremental optical encoders, HEDS-5500-A06 (*Broadcom Inc., CA, USA*), that measure the joint angle in the sagittal plane. The assistive torques are controlled using the feedback from two tensile load cells DYMH-103. The cable transmission system included two EC i-52 motors (*Maxon Group, Switzerland*). A Simulink real-time controller commands the AFO output torque. EPOS4 50/15 EtherCAT motor drivers (*Maxon Group, Switzerland*) were used to actuate motors and read the position and force feedback signals. Two snap-acting subminiature limit switches are installed on the medial and lateral sides of the AFO to control the maximum plantarflexion

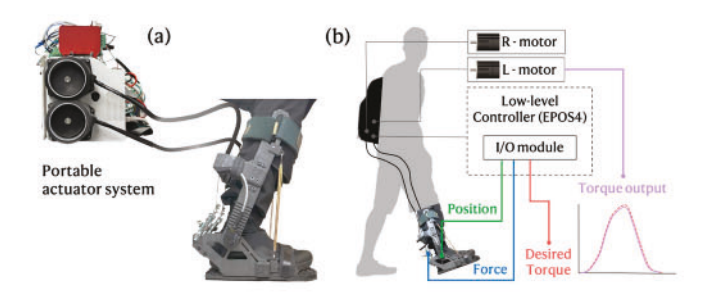


Fig. 3. (a) Portable actuator system in the off-board emulator setting with the AFO worn by a subject. (b) Schematic of the actuation system and controller.

angle for safety. To route the cable-transmission steel wires, we used Bowden cables of approximately 2 m length to carry off-board emulator testing. The diameter of the Bowden cable (5 mm) was selected to provide optimal tracking performance while minimizing the discomfort for the wearer in the portable actuation setting. The wires connect to the posterior side of the AFO's Exo-Talus utilizing a clevis rod. During the squatting activity, the reaction forces from the Bowden cables, which attach to the AFO on the posterior side of the Exo-Tibia (Fig. 3(a)), transmit the squatting torque to the subject's leg. A schematic of the controller and control hardware used to perform and control the robotic assistance is shown in Fig. 3(b). The weight of the portable actuator system is approximately 6.5 kg.

# C. Controller Design

We designed a proportional controller to regulate the assistive torques [(1)]. The desired motor velocity  $\dot{\theta}_d$  is determined by (2), where  $k_{gain}$  is the proportional gain of the torque error,  $M_d$  is the desired torque and  $M_m$  is the measured torque using the feedback from the load cell. The controller runs in Simulink (Mathworks, MA, USA) and operates at 1 KHz.

$$\dot{\theta}_d = k_{qain} \left( M_d - M_m \right) \tag{2}$$

The squat assistive torque profiles were discretized for the descent and ascent squatting phases. The torque/angle profiles were determined by the multiplication of a stiffness gain parameter and the ankle angle [29], [30]. Fig. 4 shows the assistance profiles for the four squatting conditions. The maximum torque during the ascending phase was set at 30° degree dorsiflexion ankle angle following the findings from a previous study [30]. The stiffness of descending squat was determined as a 15 Nm of plantarflexion torque at 30° degree dorsiflexion ankle angle referring to the torque boundary [30]. For the in/eversion conditions, the maximum plantar flexion torques of the left and right sides were set to 20 Nm and 6 Nm, maintaining a difference of 14 Nm between each side to achieve a 10 Nm in/eversion torque (Fig. 4(c) and (d)).

# D. Evaluation-Benchtop Test

Benchtop tests were conducted to evaluate the device's torque response time and bandwidth accuracy performance. We conducted benchtop testing on the step response and bandwidth performance by mounting the modular AFO on a built steel

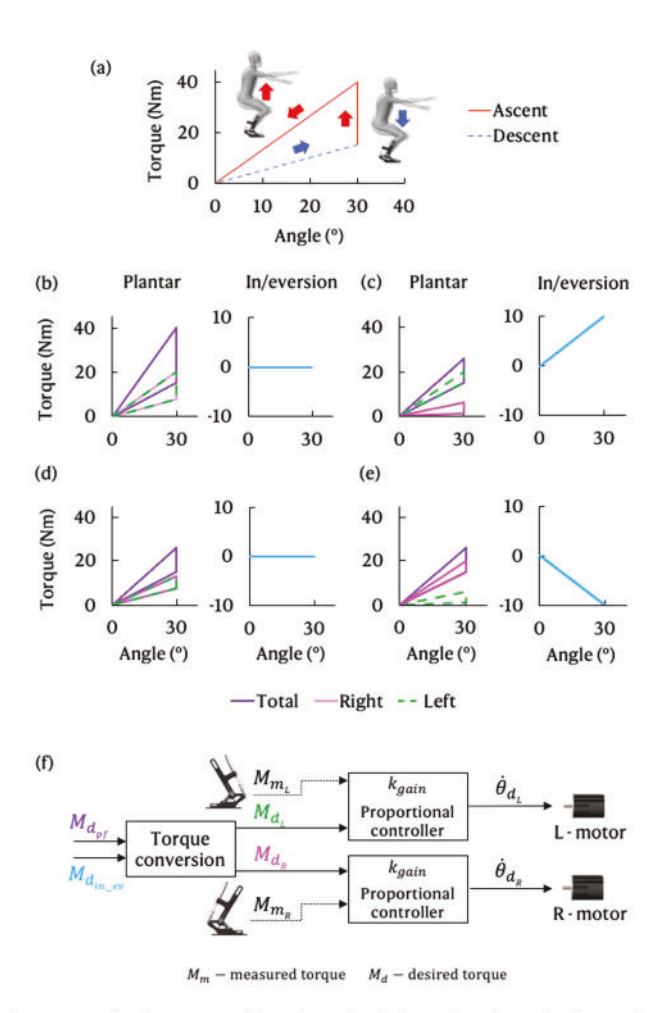


Fig. 4. Desired torque profiles; (b) and (d) show the plantarflexion and (c) and (e) the in/eversion conditions. Right and left represent the contributions from each actuator. (f) Shows how the desired controller schematic. The torque conversion block converts the desired plantar and in/eversion torque  $(M_{d_{pf}},\ M_{d_{in-ev}})$  to the desired left and right torques  $(M_{d_{L}},\ M_{d_{R}})$ . The proportional controller blocks return the motor command velocity  $(\dot{\theta}_{d_{L}},\ \dot{\theta}_{d_{R}})$  by using the desired/measured torque on left and right sides  $(M_{d_{L}},\ M_{d_{R}},\ M_{m_{L}},M_{m_{R}})$  and a proportional gain  $(k_{gain})$ .

frame using fixtures that replicate the kinematic constraints of the device when worn by a wearer. We tested up to 40 Nm for the maximum plantarflexion torque and  $\pm$  16 Nm for in/eversion. Ten trials of each condition were collected and analyzed using the mean and standard deviation. We also conducted bandwidth tests using chirp desired torque signals from 0 to 25 Hz, oscillating from 2 to 40 Nm for the plantarflexion and  $\pm$ 16 Nm for the in/eversion torques. The desired torque and measure torque signals were processed as inputs of an FFT function using MATLAB 2022a (*Mathworks, MA, USA*). To evaluate frequency response, we used the frequency where the amplitude ratio reached -3 dB and  $-180^{\circ}$  phase, indicating  $30^{\circ}$  phase margin limits at the corresponding frequency.

# E. Evaluation-AFO/Human Subject Assistance

To evaluate the device's performance during human-robot physical interaction, we conducted human-subject experiments

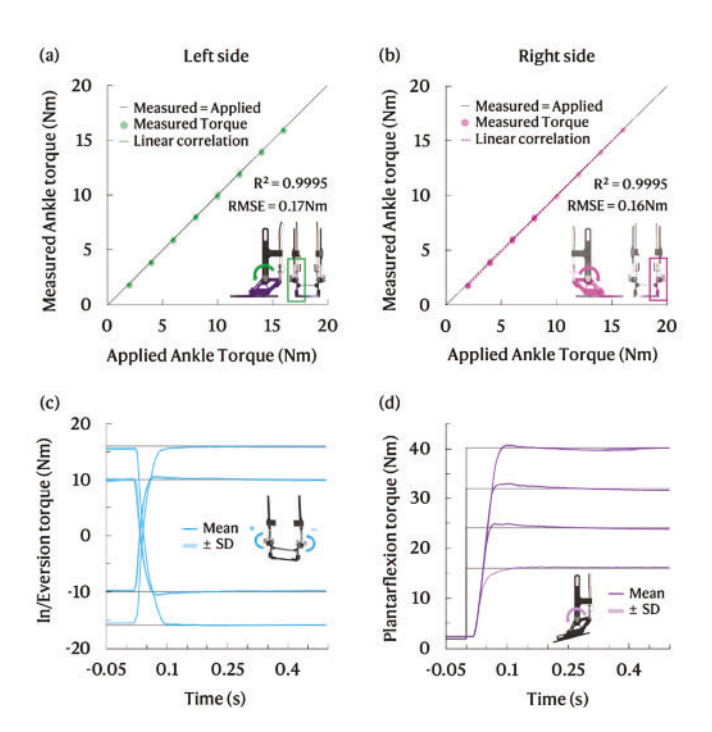


Fig. 5. (a) and (b) show the measured versus applied torque responses; (c) and (d) show the mean and standard deviation of the in/eversion and plantarflexion torque step responses, respectively.

for one subject (70 kg, 1.75 m, 35 yrs, male). The AFO's torque tracking performance was evaluated for the different assistive conditions. For the baseline condition, the subject squatted without wearing the AFO for 3 min. Then, the subject squatted wearing the AFO for five different assistive conditions: unpowered, low plantarflexion (26 Nm), high plantarflexion (40 Nm), inversion (+ 10 Nm), and eversion (-10 Nm) assistive conditions in random order (Fig. 4). During each condition, the subjects were instructed to do below parallel squats, descending until the hip joint surpasses the knee joint level in the coronal plane. The squatting cycle was divided into 1 s descent and 1 s ascent with 6 s rest standing between each squat for 3 min with a rest time between conditions of 12 min. We evaluated the AFO portable system in an off-board setting, following the disposition from a previous study using a gait assistive hip soft exosuit [31].

#### III. RESULTS AND DISCUSSION

## A. Evaluation-Benchtop Testing

The performance results evaluated the device's measured torque, response time during step response, and the closed-loop torque bandwidth. We applied plantarflexion ankle torques in steps of 2 Nm from 0 to 16 Nm for the left and right actuators, resulting in linear correlations ( $R^2 = 0.9995$ ) between the measured and applied torque with root mean square errors of 0.17 Nm for the left side (Fig. 5(a)) and 0.16 Nm for the right side (Fig. 5(b)). The torque measurement accuracy is comparable to a previous 1-DOF ankle exoskeleton with an RMS error of 0.13 Nm [32] (Table I).

TABLE I
TORQUE TRACKING RMS ERRORS OF THE MEASURED VERSUS DESIRED
TORQUES CORRESPONDING TO THE DIFFERENT SQUATTING CONDITIONS

		exion Torque acking	In/Eversion Torque Tracking		
Assistance condition	RMS error (Nm)	Mean RMS error (Nm)	RMS error (Nm)	Mean RMS error (Nm)	
$M_{pf} = 26 \text{ Nm}$	$1.8 \pm 0.6$	1.8	$1.8 \pm 0.6$	0.1	
$M_{\rm pf} = 40 \text{ Nm}$	$2.0 \pm 1.1$	2.2	$1.8 \pm 0.6$	0.3	
$M_{in} = 10 \text{ Nm}$	$2.8 \pm 1.2$	3.0	$0.6 \pm 0.4$	0.7	
$M_{ev} = 10 \text{ Nm}$	$2.9 \pm 1.2$	3.0	$0.7 \pm 0.5$	0.8	

RMS errors represent the error through the entire trial and mean RMS error represents the mean error for the squatting cycle.

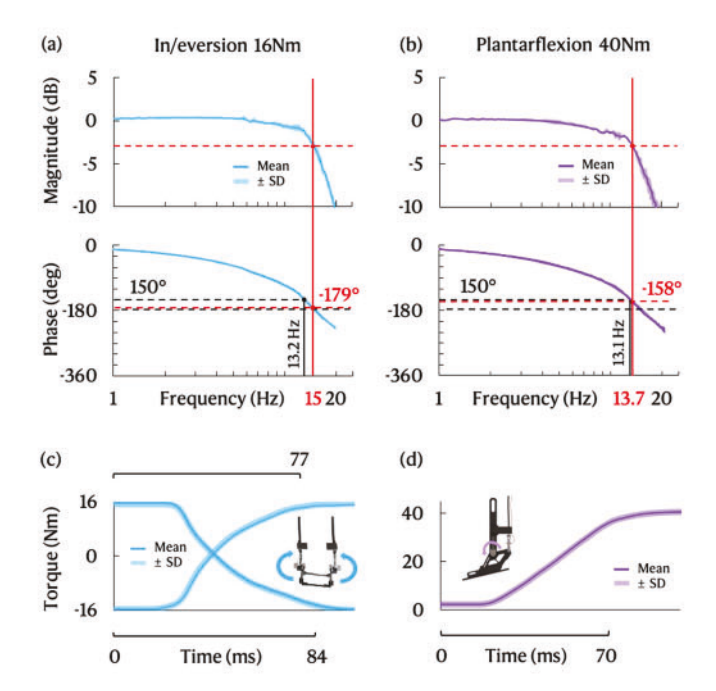


Fig. 6. (a) and (b) are the frequency response results; (c) and (d) are the step response time results.

Fig. 5(c) and (d) presents the mean and standard deviation of the step response for the in/eversion (mean overshoot of  $0.83 \pm 0.38\%$  for  $\pm 10$  Nm) and plantarflexion torques ( $1.79 \pm 0.34\%$  at the maximum torque of 40 Nm). The mean response time corresponding to a 90% rise time for the maximum in/eversion torque step response between -16 Nm and 16 Nm was  $77.5 \pm 0.8$  ms and  $84.1 \pm 0.6$  ms, respectively (Fig. 6(c)). For the maximum 40 Nm plantarflexion torque, the mean response time was  $70 \pm 0.6$  ms (Fig. 6(d)). Our device response time in the two degrees of freedom performs exceptionally fast compared to the reported response time of previously wearable robots, with plantarflexion response times greater than 200 ms [33] and 1000 ms [34].

The device's bandwidth frequency to an in/eversion torque of  $\pm$  16 Nm for a -3 dB magnitude was 15 Hz, with a  $-179^{\circ}$  phase (Fig. 6(a)). For a 30° phase margin, the frequency was 13.2 Hz. The bandwidth frequency under 40 Nm plantarflexion torque was 13.7 Hz, corresponding to a  $-158^{\circ}$  phase (Fig. 6(b)). For a

30° phase margin, the frequency was 13.1 Hz. Stationary cable-driven ankle exoskeletons have reported closed-loop bandwidths between 17.7 Hz to 24.2 Hz for plantarflexion torques ranging from 20 Nm to 50 Nm [24], [32]. The developed modular AFO with 2-DOF exhibited comparable bandwidth for both plantar and in/eversion torques.

## B. Evaluation-AFO/Human Subject Assistance

We evaluated the torque tracking performance of the AFO during human-subject squatting experiments. We analyzed the mean trajectories for the desired and measured torques during descent and ascent squatting (Fig. 7). Two RMS errors were calculated for the assistive torque, one for the entire squatting trial for each condition and the other for the mean squatting cycle (Mean RMS error), as outlined in Table II. The RMS error during the plantarflexion conditions was  $1.8 \pm 0.6$  Nm and  $2.0 \pm 1.1$  Nm for 26 and 40 Nm, respectively. The AFO tracking performance during squatting is similar to cable-driven ankle exoskeletons with plantarflexion assistance during walking, which reported RMS errors of 1.7  $\pm$  0.6 Nm and 2.0  $\pm$  0.5 Nm for maximum plantarflexion torques of  $\sim 70$  Nm [32] and 0.51 Nm for 54 Nm [35]. The in/eversion torque conditions resulted in errors of  $0.6 \pm 0.4$  Nm and  $0.7 \pm 0.5$  Nm for 10 Nm in/eversion. The in/eversion tracking performance was similar to that of the anklefoot prosthesis, which has shown RMS errors ranging from 0.3 -0.7 Nm during walking with  $\pm$  15 Nm in/eversion assistive

Various studies have developed wearable exoskeletons and exosuits for ankle joint assistance with plantarflexion torques ranging from 5.6 to 120 Nm [23], [24], [26], [27], [32], [33], [34], [35], [36], [37] (Table II). Cable-driven actuation systems average maximum plantarflexion of 38.3  $\pm$  38.9 Nm [23], [24], [26], [27], [32], [35], [37], where portable cable-driven AFO average  $25.5 \pm 18.1$  Nm [23], [26], [27], [35], [37]. In this study, we developed 2-DOF modular AFO, the first portable cabledriven AFO that provides in/eversion torque assistance up to 16 Nm, and it can also provide a maximum plantarflexion torque of 40 Nm. Although a pneumatic AFO can provide in/eversion torque assistance up to 21 Nm, our AFO offers a greater range of motion and a faster response time [33] (Table II). The worn weight of the AFO (0.9 kg) is also within the light portable cable-driven ankle exoskeletons, which range from 0.9 to 2.9 kg [23], [26], [35], [37], [38], [39], [40].

Future work will evaluate the AFO under different activities, including walking, and for a larger sample size. To use the device during walking, the implementation of a gait event recognition system will be implemented using force-sensing resistors located at the sole [41]. The in/eversion assistance from the AFO could help improve muscle strength and balance during training in people with chronic stroke [9]. We will evaluate the device in populations with reduced mobility during gait and daily activities. Real-time visual biofeedback and motion capture system will be used to help the subject control the knee flexion angle during sit-to-stand. The total weight of the portable emulator system (6.5kg) is in the range of AFO portable actuation systems (1.65 to 10.1 kg [23], [26], [35], [37]). However,

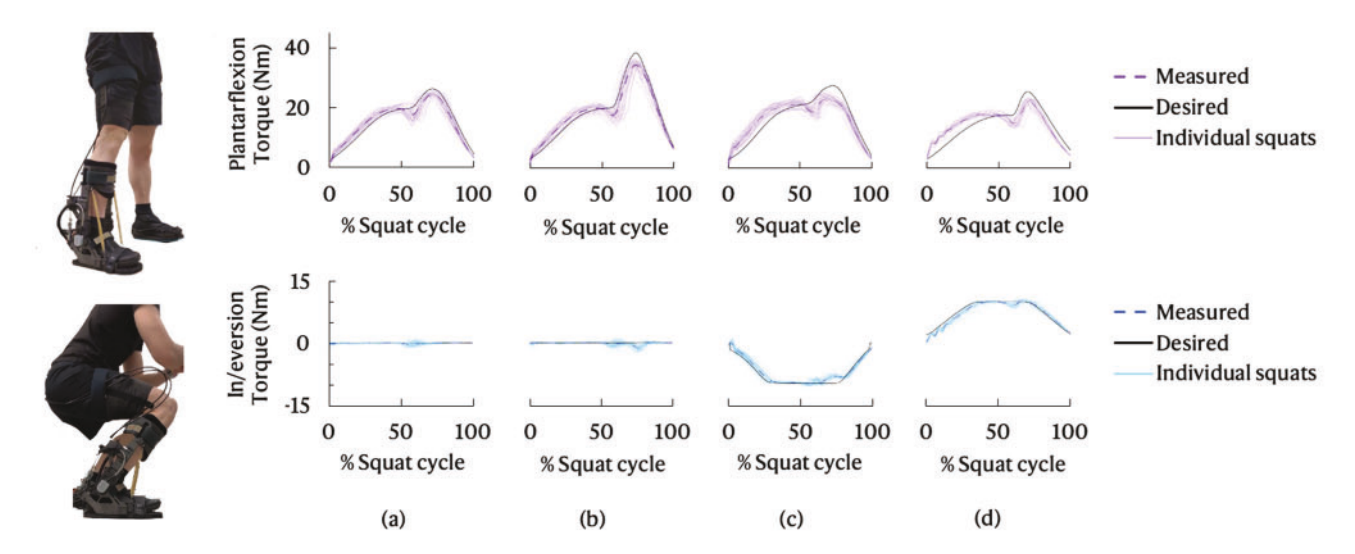


Fig. 7. Torque tracking profiles for the different assistance conditions during squatting; (a) and (b) are the plantarflexion (top row) and in/eversion (bottom row) torque profiles for the low (26 Nm) and high plantarflexion conditions (40 Nm), respectively; (c) and (d) are the eversion and inversion conditions.

TABLE II							
WEARARI E ANKLE ROBOTS' CAPABILITIES COMPARISON							

Actuation	DOF Active/Passive	Dorsi ROM (°)	flexion Torque (Nm)	Planta ROM (°)	Torque (Nm)	Inversion ROM	on/eversion Torque (Nm)	Response time (ms) pf / in/ev	Freq.	Weight (kg) AFO / total	Reference
P-CD	2/2	40	1.51	25	40	±25	0 - 16	70 / 84	14-15	0.9 / 6.5	This study
P-CD	1/2	>20	-	30	54	100	NA	1.0	15	1.2 / 1.7	[35]
P-P	1/2	>20	1.70	30	~ 70	-	NA	> 200 / -	0.00	0.2	[33]
S-CD	1/2	>20	-	30	120	-	NA	-	18-24	0.8	[32]
P-CD	1/2	-	5.6	2.0	5.6	-	NA	-	5. <b>-</b> 5	1.5	[26]
P-CD	1/3	>20	~ 24	> 30	~ 24	-	NA	-	: <del>-</del>	~ 0.9 / 3.8	[23]
P-DD	1/1	>20	-	>20	16.7	-	NA	-	-	0.5 / 1	[36]
P-CD	1/3	-	-	> 30	28	-	NA	-		-	[27]
P-CD	1/3	>20	180	> 30	16	-	NA	.= 1	-	2 / 10.1	[37]
S-CD	1/3	>20	123	> 30	20.4	12	NA	-	3-20	=	[24]
P-P	2/3	14	110	13	53	±10	0 - 21	> 1000 / -	-	-	[34]
S-DD	1/1	~ 12	121	30	21	-	NA	-	12	0.8	[38]
P-DD	1 / 1	2	-	-	53	12	NA	> 70 / -	32	2.9	[39]
P-DD	1/1	>20	126	20	35	12	NA	125	59 <b>2</b> 6	0.7 / 1.3	[40]

P-CD: Portable driven; P-P: Portable pneumatic; S-CD: Stationary cable driven; P-DD: Portable direct drive; pf: Plantarflexion; in/ev: inversion/eversion; NA: no assistance.

compared to stationary systems, our compact design could allow easy ambulatory use in clinical applications. Future work will investigate optimizing the total weight of the portable system to translate applications in an outdoor setting. We will also investigate improving the AFO-human interface attaching to the subject's foot to minimize the possibility of misalignment during the use of the device by using a strapping system that connects to a larger area of the foot on the anterior and posterior side while maintaining comfort.

## IV. CONCLUSION

This study presented an additively manufactured modular robotic Ankle-Foot Orthosis (AFO) with an integrated portable actuator system. The maximum torque capabilities and degrees of assistance are improved compared to conventional rigid AFO using off-board systems. Our design offers a cost-effective wearable robot with inversion/eversion assistance capabilities. Results from benchtop and human-subject experiments indicate suitable maximum torque and control bandwidth, resulting in reasonable torque tracking performance. Moreover, the AFO has in/eversion torque assistance capabilities not seen in other wearable ankle robots using direct drive and cable-driven actuation systems. The in/eversion response time was improved compared to previous wearable ankle robots driven by pneumatic actuators. The modular design allows personalization to match the wearer's foot size and leg length characteristics. The device could be used in potential applications developing personalized ankle exoskeletons and studying the effects of in/eversion in injury risk mitigation and balance enhancement during various activities

such as walking and sit-to-stand, thereby improving mobility in older adult groups with reduced ankle strength and stability.

#### ACKNOWLEDGMENT

The authors thank Aditya Patel and Andrés Valverde for helping during the manufacturing and assembly of the AFO components and Prakyath Kantharaju for helping prepare the equipment and materials during data collection. The authors also thank Anchi He and Kishan Patel for their guidance regarding the portable actuator setup.

*Declarations:* This study was performed in line with the principles of the Declaration of Helsinki. Approval was granted by the Institutional Review Board, The University of Illinois at Chicago. (Protocol 2020–0563).

#### REFERENCES

- T. Vos and S. S. Lim, "Global burden of 369 diseases and injuries in 204 countries and territories, 1990–2019: A systematic analysis for the global burden of disease study 2019," *Lancet*, vol. 396, no. 10258, pp. 1204–1222, 2020, doi: 10.1016/S0140-6736(20)30925-9.
- [2] P. W. Duncan et al., "Management of adult stroke rehabilitation care: A clinical practice guideline," Stroke, vol. 36, no. 9, Sep. 2005, Art. no. e100-43, doi: 10.1161/01.STR.0000180861.54180.FF.
- [3] C. J. L. Murray et al., "Disability-adjusted life years (DALYs) for 291 diseases and injuries in 21 regions, 1990–2010: A systematic analysis for the global burden of disease study 2010," *Lancet*, vol. 380, no. 9859, pp. 2197–2223, 2012.
- [4] A. Guzik, M. Drużbicki, and A. Wolan-Nieroda, "Assessment of two gait training models: Conventional physical therapy and treadmill exercise, in terms of their effectiveness after stroke," *Hippokratia*, vol. 22, no. 2, pp. 51–59, 2018.
- [5] J. Mehrholz, M. Pohl, and B. Elsner, "Treadmill training and body weight support for walking after stroke," *Cochrane Database Syst. Rev.*, vol. 2014, no. 1, Jan. 2014, Art. no. CD002840, doi: 10.1002/14651858.CD002840.pub3.
- [6] M. Sivan, R. J. O'Connor, S. Makower, M. Levesley, and B. Bhakta, "Systematic review of outcome measures used in the evaluation of robotassisted upper limb exercise in stroke," *J. Rehabil. Med.*, vol. 43, no. 3, pp. 181–189, Feb. 2011, doi: 10.2340/16501977-0674.
- [7] G. Morone et al., "Robot-assisted gait training for stroke patients: Current state of the art and perspectives of robotics," *Neuropsychiatric Dis. Treat.*, vol. 13, pp. 1303–1311, 2017, doi: 10.2147/NDT.S114102.
- [8] M. Belas Dos Santos, C. Barros de Oliveira, A. Dos Santos, C. Garabello Pires, V. Dylewski, and R. M. Arida, "A comparative study of conventional physiotherapy versus robot-assisted gait training associated to physiotherapy in individuals with ataxia after stroke," *Behav. Neurol.*, vol. 2018, 2018, Art. no. 2892065, doi: 10.1155/2018/2892065.
- [9] B. Shi et al., "Wearable ankle robots in post-stroke rehabilitation of gait: A systematic review," Front. Neurorobot., vol. 13, 2019, Art. no. 63, doi: 10.3389/fnbot.2019.00063.
- [10] A. K. Blanchette, M. Noël, C. L. Richards, S. Nadeau, and L. J. Bouyer, "Modifications in ankle dorsiflexor activation by applying a torque perturbation during walking in persons post-stroke: A case series," *J. Neuroeng. Rehabil.*, vol. 11, no. 1, 2014, Art. no. 98, doi: 10.1186/1743-0003-11-98.
- [11] K. Z. Takahashi, M. D. Lewek, and G. S. Sawicki, "A neuromechanics-based powered ankle exoskeleton to assist walking post-stroke: A feasibility study," *J. Neuroeng. Rehabil.*, vol. 12, no. 1, 2015, Art. no. 23, doi: 10.1186/s12984-015-0015-7.
- [12] L.-F. Yeung et al., "Randomized controlled trial of robot-assisted gait training with dorsiflexion assistance on chronic stroke patients wearing ankle-foot-orthosis," J. Neuroeng. Rehabil., vol. 15, no. 1, 2018, Art. no. 51, doi: 10.1186/s12984-018-0394-7.
- [13] M. Kim and S. H. Collins, "Step-to-step ankle inversion/eversion torque modulation can reduce effort associated with balance," *Front. Neurorobot.*, vol. 11, 2017, Art. no. 62, doi: 10.3389/fnbot.2017.00062.
- [14] J. Zhang et al., "Human-in-the-loop optimization of exoskeleton assistance during walking," *Science*, vol. 356, no. 6344, pp. 1280–1284, Jun. 2017, doi: 10.1126/science.aal5054.

- [15] Y. Ding, M. Kim, S. Kuindersma, and C. J. Walsh, "Human-in-the-loop optimization of hip assistance with a soft exosuit during walking," Sci. Robot., vol. 3, no. 15, 2018, Art. no. eaar5438, doi: 10.1126/scirobotics.aar5438.
- [16] K. A. Shorter, J. Xia, E. T. Hsiao-Wecksler, W. K. Durfee, and G. F. Kogler, "Technologies for powered ankle-foot orthotic systems: Possibilities and challenges," *IEEE/ASME Trans. Mechatronics*, vol. 18, no. 1, pp. 337–347, Feb. 2013, doi: 10.1109/TMECH.2011.2174799.
- [17] C. Lagoda, J. C. Moreno, and J. L. Pons, "Human-robot interfaces in exoskeletons for gait training after stroke: State of the art and challenges," *Appl. Bionics Biomech.*, vol. 9, pp. 193–203, 2012, doi: 10.3233/ABB-2012-0056.
- [18] I. Sanz-Pena, J. Blanco, and J. H. Kim, "Computer interface for real-time gait biofeedback using a wearable integrated sensor system for data acquisition," *IEEE Trans. Hum.-Mach. Syst.*, vol. 51, no. 5, pp. 484–493, Oct. 2021, doi: 10.1109/THMS.2021.3090738.
- [19] S.-K. Bok, T. H. Lee, and S. S. Lee, "The effects of changes of ankle strength and range of motion according to aging on balance," *Ann. Rehabil. Med.*, vol. 37, no. 1, pp. 10–16, Feb. 2013, doi: 10.5535/arm.2013.37.1.10.
- [20] A. F. Ambrose, G. Paul, and J. M. Hausdorff, "Risk factors for falls among older adults: A review of the literature," *Maturitas*, vol. 75, no. 1, pp. 51–61, May 2013, doi: 10.1016/j.maturitas.2013.02.009.
- [21] Y. J. Shin, S. M. Kim, and H. S. Kim, "Immediate effects of ankle eversion taping on dynamic and static balance of chronic stroke patients with foot drop," J. Phys. Ther. Sci., vol. 29, no. 6, pp. 1029–1031, Jun. 2017, doi: 10.1589/jpts.29.1029.
- [22] S. Ramadurai, H. Jeong, and M. Kim, "Predicting the metabolic cost of exoskeleton-assisted squatting using foot pressure features and machine learning," Front. Robot. AI, vol. 10, 2023, Art. no. 1166248, doi: 10.3389/frobt.2023.1166248.
- [23] J. Bae et al., "A lightweight and efficient portable soft exosuit for paretic ankle assistance in walking after stroke," in *Proc. IEEE Int. Conf. Robot. Automat.*, 2018, pp. 2820–2827, doi: 10.1109/ICRA.2018.8461046.
- [24] Y. Ding, I. Galiana, A. Asbeck, B. Quinlivan, S. M. M. De Rossi, and C. Walsh, "Multi-joint actuation platform for lower extremity soft exosuits," in *Proc. IEEE Int. Conf. Robot. Automat.*, 2014, pp. 1327–1334, doi: 10.1109/ICRA.2014.6907024.
- [25] M. Kim, T. Chen, T. Chen, and S. H. Collins, "An ankle-foot prosthesis emulator with control of plantarflexion and inversion-eversion torque," *IEEE Trans. Robot.*, vol. 34, no. 5, pp. 1183–1194, Oct. 2018, doi: 10.1109/TRO.2018.2830372.
- [26] J. Kwon, J.-H. Park, S. Ku, Y. Jeong, N.-J. Paik, and Y.-L. Park, "A soft wearable robotic ankle-foot-orthosis for post-stroke patients," *IEEE Robot. Automat. Lett.*, vol. 4, no. 3, pp. 2547–2552, Jul. 2019, doi: 10.1109/LRA.2019.2908491.
- [27] F. A. Panizzolo et al., "A biologically-inspired multi-joint soft exosuit that can reduce the energy cost of loaded walking," J. Neuroeng. Rehabil., vol. 13, no. 1, 2016, Art. no. 43, doi: 10.1186/s12984-016-0150-9.
- [28] S. H. Collins, M. Kim, T. Chen, and T. Chen, "An ankle-foot prosthesis emulator with control of plantarflexion and inversion-eversion torque," in *Proc. IEEE Int. Conf. Robot. Automat.*, 2015, pp. 1210–1216, doi: 10.1109/ICRA.2015.7139345.
- [29] H. Jeong, P. Haghighat, P. Kantharaju, M. Jacobson, H. Jeong, and M. Kim, "Muscle coordination and recruitment during squat assistance using a robotic ankle-foot exoskeleton," *Sci. Rep.*, vol. 13, no. 1, 2023, Art. no. 1363, doi: 10.1038/s41598-023-28229-4.
- [30] P. Kantharaju, H. Jeong, S. Ramadurai, M. Jacobson, H. Jeong, and M. Kim, "Reducing squat physical effort using personalized assistance from an ankle exoskeleton," *IEEE Trans. Neural Syst. Rehabil. Eng.*, vol. 30, pp. 1786–1795, 2022, doi: 10.1109/TNSRE.2022.3186692.
- [31] G. Lee, Y. Ding, I. G. Bujanda, N. Karavas, Y. M. Zhou, and C. J. Walsh, "Improved assistive profile tracking of soft exosuits for walking and jogging with off-board actuation," in *Proc. IEEE/RSJ Int. Conf. Intell. Robots Syst.*, 2017, pp. 1699–1706, doi: 10.1109/IROS.2017.8205981.
- [32] K. A. Witte, J. Zhang, R. W. Jackson, and S. H. Collins, "Design of two lightweight, high-bandwidth torque-controlled ankle exoskeletons," in *Proc. IEEE Int. Conf. Robot. Automat.*, 2015, pp. 1223–1228, doi: 10.1109/ICRA.2015.7139347.
- [33] C. M. Thalman, M. Debeurre, and H. Lee, "Entrainment during human locomotion using a soft wearable ankle robot," *IEEE Robot. Automat. Lett.*, vol. 6, no. 3, pp. 4265–4272, Jul. 2021, doi: 10.1109/LRA.2021.3066961.
- [34] Y.-L. Park et al., "Design and control of a bio-inspired soft wearable robotic device for ankle-foot rehabilitation," *Bioinspiration Biomimetics*, vol. 9, no. 1, Mar. 2014, Art. no. 16007, doi: 10.1088/1748-3182/9/1/016007.

- [35] P. Slade, M. J. Kochenderfer, S. L. Delp, and S. H. Collins, "Personalizing exoskeleton assistance while walking in the real world," *Nature*, vol. 610, no. 7931, pp. 277–282, 2022, doi: 10.1038/s41586-022-05191-1.
- [36] L.-F. Yeung et al., "Design of an exoskeleton ankle robot for robot-assisted gait training of stroke patients," in *Proc. IEEE Int. Conf. Rehabil. Robot.*, 2017, pp. 211–215, doi: 10.1109/ICORR.2017.8009248.
- [37] A. T. Asbeck, S. M. M. De Rossi, K. G. Holt, and C. J. Walsh, "A biologically inspired soft exosuit for walking assistance," *Int. J. Robot. Res.*, vol. 34, no. 6, pp. 744–762, 2015, doi: 10.1177/0278364914562476.
- [38] C. Wang et al., "Design of an ankle exoskeleton that recycles energy to assist propulsion during human walking," *IEEE Trans. Biomed. Eng.*, vol. 69, no. 3, pp. 1212–1224, Mar. 2022, doi: 10.1109/TBME.2021.3120716.
- [39] B. DeBoer, A. Hosseini, and C. Rossa, "A discrete non-linear series elastic actuator for active ankle-foot orthoses," *IEEE Robot. Automat. Lett.*, vol. 7, no. 3, pp. 6211–6217, Jul. 2022, doi: 10.1109/LRA.2022.3167065.
- [40] J. Taborri et al., "RANK-robotic ankle: Design and testing on irregular terrains," in *Proc. IEEE/RSJ Int. Conf. Intell. Robots Syst.*, 2022, pp. 9752–9757, doi: 10.1109/IROS47612.2022.9981580.
- [41] C. M. Thalman, T. Hertzell, and H. Lee, "Toward a soft robotic ankle-foot orthosis (SR-AFO) exosuit for human locomotion: Preliminary results in late stance plantarflexion assistance," in *Proc. IEEE 3rd Int. Conf. Soft Robot.*, 2020, pp. 801–807, doi: 10.1109/RoboSoft48309.2020.9116050.